ACS Catalysis

Letter

pubs.acs.org/acscatalysis

Tips-Bundled Pt/Co_3O_4 Nanowires with Directed Peripheral Growth of Li_2O_2 as Efficient Binder/Carbon-Free Catalytic Cathode for Lithium−Oxygen Battery

Jingyi Cao,[†] Shuangyu Liu,[†] Jian Xie,*[,†,‡] Shichao Zhang,[§] Gaoshao Cao,[‡] and Xinbing Zhao*[,†,‡]

[†]State Key Laboratory of Silicon Materials, Department of Materials Science and Engineering, Zhejiang University, Hangzhou 310027, China

[‡]Key Laboratory of Advanced Materials and Applications for Batteries of Zhejiang Province, Hangzhou 310027, China

[§]School of Materials Science and Engineering, Beijing University of Aeronautics and Astronautics, Beijing 100191, China

Supporting Information

ABSTRACT: We propose a new design of a binder/carbon-free air electrode with tips-bundled Pt/Co_3O_4 nanowires grown directly on Ni foam substrate. In this design, the side reactions related to binder/carbon are excluded. The presence of Pt not only promotes the formation of the tips-bundled structure of Co_3O_4 nanowires but also directs the uniform deposition of a fluffy, thin Li_2O_2 layer only on the periphery of Pt/Co_3O_4 nanowires. This crystallization habit of Li_2O_2 makes it easy to decompose upon recharge with reduced side reactions. As a result, Li−O_2 batteries with this cathode show low polarization.

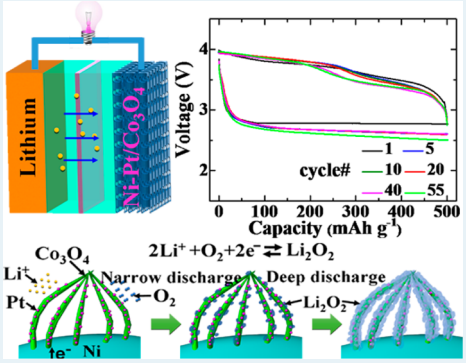

KEYWORDS: *lithium−oxygen batteries, cobalt oxide, platinum, tips-bundled nanowires, binder/carbon free, directed Li_2O_2 growth*

Li−O_2 (Li−air) batteries can provide a theoretical energy density of 3505 Wh kg^{-1}, which is greatly higher than the current Li-ion batteries, for instance 584 Wh kg^{-1} for $LiCoO_2$/C system.[1−5] Despite recent advances, where long-term cycling of Li−O_2 battery could be achieved,[6−8] great challenges still remain to develop practical Li−O_2 batteries. The performance of the Li−O_2 battery is largely limited by the inherent drawbacks of Li_2O_2, the discharge product. One disadvantage of Li_2O_2 is its rather low electric conductivity.[9] The accumulation of insulating Li_2O_2 will unavoidably passivate the electrode. This barrier can be partly overcome by directing the growth of Li_2O_2 on conductive matrices, usually carbon materials decorated with noble metal catalysts.[10−12] Another disadvantage of Li_2O_2 (or its intermediate LiO_2) is its high reactivity toward the carbon matrix, electrolyte, and binder.[13−16] The parasitic reactions will lead to the formation of undesirable byproducts (e.g., Li_2CO_3) and the accumulation of the byproducts on cycling will result in performance degradation and eventual failure of the battery.[14−16]

Considering the above facts, both material and architecture of the catalytic cathode should be optimized to alleviate the negative effect of Li_2O_2. Growing catalyst directly on a metallic substrate could avoid the use of conductive carbon and binder,[17] thus reducing the side reactions. The electrode deactivation could be effectively relieved and delayed by directing the growth of Li_2O_2 into a favorable form (e.g., thin, small size) and onto a conductive matrix via precious metals.[10−12] However, the reported matrices are limited to carbon materials,[10−12] which are unstable in the presence of Li_2O_2 (or LiO_2)[14−16] and also catalyze the electrolyte decomposition.[15] Therefore, metal oxides were suggested to act as support for precious metals since they are more stable against the attack of Li_2O_2 (or LiO_2) than carbon materials.[17,18] In this regard, oxides with good catalytic activity, such as Co_3O_4,[19−21] $NiCo_2O_4$,[22,23] MnO_2,[24−27] and Fe_2O_3,[28] are favorable.

In this work, we report a new design of binder/carbon-free catalytic cathode by growing tips-bundled Pt/Co_3O_4 nanowires directly onto Ni foam. This electrode design excludes the binder/carbon involved side reactions. The presence of Pt not only promotes the formation of the unique tips-bundled structure of Co_3O_4 nanowires, but also directs the uniform deposition of a fluffy, thin Li_2O_2 layer only on the periphery of Pt/Co_3O_4 nanowires. The tips-bundled Pt/Co_3O_4 nanowires are mechanically strong to support Li_2O_2. Co_3O_4 is selected as the support for Pt because it can grow directly onto the metal substrate and into nanowires form via a facile hydrothermal route, besides its good catalytic activity for Li−O_2 batteries.[19−21] The Pt/Co_3O_4 exhibits superior catalytic effect for

Received: September 15, 2014
Revised: November 28, 2014
Published: December 2, 2014

 © 2014 American Chemical Society

Li−O_2 battery due to its unique design in both structure and component. The architecture and working mechanism of the Li−O_2 battery with Ni foam supported Pt/Co_3O_4 catalytic cathode are shown in Figure 1.

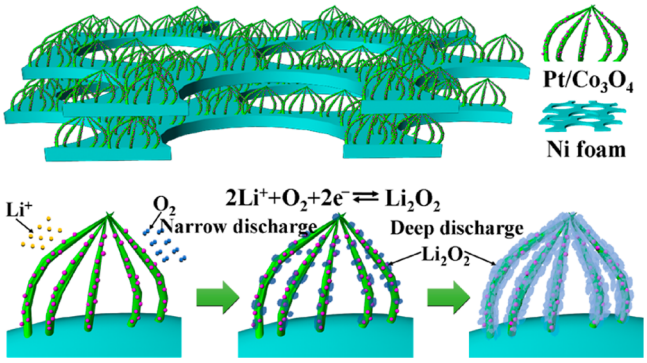

Figure 1. Schematic illustration of the architecture and working mechanism of Li−O_2 battery with Ni foam supported Pt/Co_3O_4 cathode.

The growth of Pt/Co_3O_4 nanowires on Ni foam was realized by a facile hydrothermal route (Experimental Section, Supporting Information). Figure 2a shows the X-ray diffraction (XRD) patterns of Pt/Co_3O_4 and Co_3O_4 supported on Ni foam. XRD patterns indicate the formation of Pt/Co_3O_4 and Co_3O_4. The formation of Co_3O_4 for both samples was also confirmed by X-ray photoelectron spectra (XPS, Figure S1). The weight ratio of Pt to Co_3O_4 is around 1:39, corresponding to Pt/Co molar ratio of 1:95. Scanning electron microscopy (SEM) images in Figure 2b demonstrate that Pt/Co_3O_4 was deposited only on the skeleton of Ni foam, copying its three-dimensional (3D) interconnected scaffold structure, while the large pores of Ni foam are kept intact. As seen in Figure 2c, slender Pt/Co_3O_4 nanowires with sharp tips are uniformly and orderly arranged on Ni foam. Typical Pt/Co_3O_4 nanowires have a diameter below 200 nm and a length of several microns. Of note is that the tips of the nanowires are bundled together, which is mechanically more stable to support the reaction product. The polycrystalline feature of a single Pt/Co_3O_4 nanowire is revealed by transmission electron microscopy (TEM, Figure 2d,e). High-resolution TEM (HRTEM) image in Figure 2e indicates that Pt nanocrystals with a size below 5 nm are homogeneously distributed in Co_3O_4 nanowire. For bare Co_3O_4, although it also exhibits a nanowire shape with a similar size, the tips-bundled feature is hardly seen and the nanowires show a random arrangement on Ni foam substrate as shown in Figure 2f. It suggests that the presence of Pt promotes the formation of the novel tips-bundled structure and orderly arrangement of Co_3O_4 nanowires. It suggests that the loading of Pt can change the center of gravity of Co_3O_4 nanowires, making the nanowires incline toward the same direction, while the Pt induced recrystallization makes the tips of nanowires bundle together.

The electrocatalytic activity of Pt/Co_3O_4 was investigated in Li−O_2 batteries and compared with that of bare Co_3O_4. The specific current and capacity are normalized by the total mass of catalyst on the Ni foam. Figure 3a compares the first discharge−charge curves of Li−O_2 batteries with Ni foam supported Pt/Co_3O_4 and Co_3O_4 cathodes at 100 mA g^{-1}. Li−O_2 batteries with Pt/Co_3O_4 and Co_3O_4 catalysts deliver discharge capacities of 1371 and 1348 mAh g^{-1}, respectively. Note that Pt/Co_3O_4 catalyzed Li−O_2 battery exhibits an obviously lower midcapacity overpotential (defined as the overpotential at half capacity, 1.12 V) than Co_3O_4 catalyzed one (1.48 V) even though the former is deposited more insulating Li_2O_2 after discharge. Considering the fact that the decrease in polarization occurs mainly in the charge process, it is thus expected that Pt may induce the crystallization Li_2O_2 into a favorable form which is easier to decompose upon recharge.

The cycling performance of Li−O_2 batteries with Pt/Co_3O_4 and Co_3O_4 cathodes was evaluated by galvanostatic cycling at

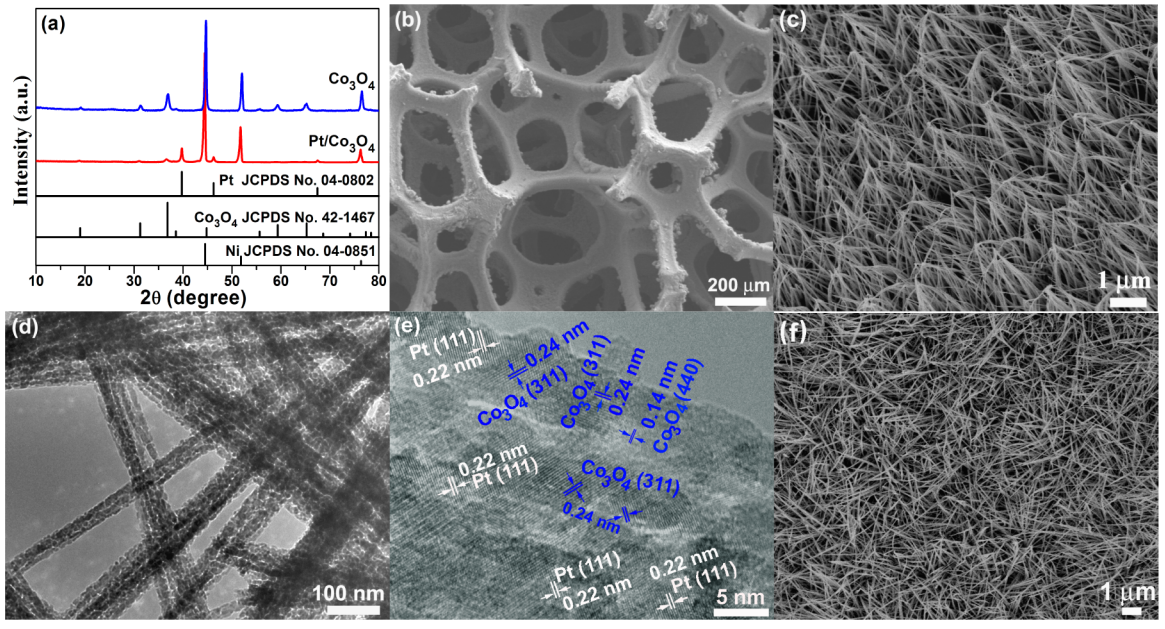

Figure 2. (a) XRD patterns of Pt/Co_3O_4 and Co_3O_4 on nickel foam, (b,c) SEM images of Pt/Co_3O_4 on Ni foam, (d) TEM and (e) HRTEM images of the sample from Ni foam supported Pt/Co_3O_4, and (f) SEM image of Co_3O_4 on nickel foam.

dx.doi.org/10.1021/cs501392p | ACS Catal. 2015, 5, 241−245

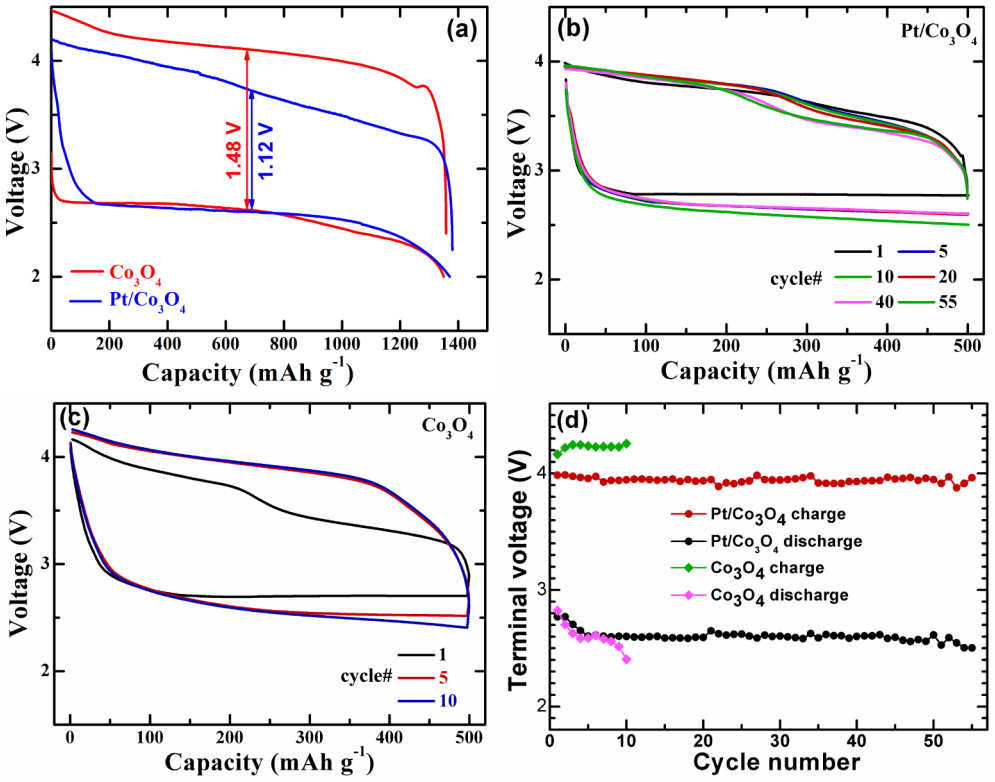

Figure 3. (a) First voltage profiles of Li−O_2 batteries with Pt/Co_3O_4 and Co_3O_4 cathode at 100 mA g^{-1}, (b,c) voltage profiles, and (d) terminal voltages of Li−O_2 batteries with Pt/Co_3O_4 and Co_3O_4 cathodes under 100 mA g^{-1} at a limited capacity of 500 mAh g^{-1}.

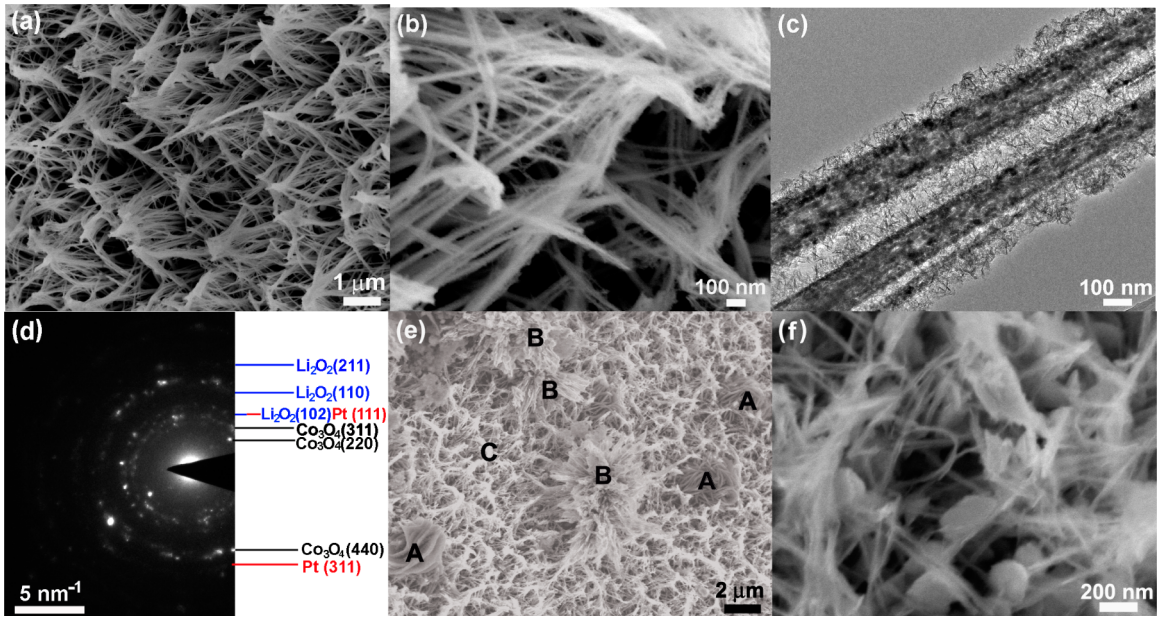

Figure 4. (a,b) SEM images of Ni foam supported Pt/Co_3O_4 electrode after the first discharge to 500 mAh g^{-1}, (c) TEM images and (d) SAED patterns of the sample from the Pt/Co_3O_4 electrode after the first discharge to 500 mAh g^{-1}, and (e,f) SEM images of Ni foam supported Co_3O_4 cathode after the first discharge to 500 mAh g^{-1}.

100 mA g^{-1} with the capacity limited at 500 mAh g^{-1}. As shown in Figure 3b, the first discharge plateau of Pt/Co_3O_4 catalyzed battery is 2.80 V and is stabilized at >2.50 V up to 55 cycles. The charge curves exhibit two plateaus at 3.6 and 3.9 V, indicating the two-step decomposition of Li_2O_2. A possible explanation for the two-step delithiation is that thin Li_2O_2 deposits can decompose at low potentials through electron tunneling, while thick Li_2O_2 deposits decompose at high potentials through polaron hopping.[29] This phenomenon, however, can hardly be seen for the Co_3O_4 catalyzed battery apart from the first charge (Figure 3c). Figure 3d also indicates that the formed Li_2O_2 can be completely decomposed below 4.0 V during 55 cycles. This is favorable since high charge potential will unavoidably lead to undesirable side reactions, for

dx.doi.org/10.1021/cs501392p | ACS Catal. 2015, 5, 241−245

instance electrolyte decomposition.[30] Pt/Co_3O_4 catalyzed battery can sustain a cycling for 55 times. For the Co_3O_4 catalyzed battery, in contrast, the cycling can last only 10 cycles with high charge end voltages (>4.0 V) and low discharge end voltages (<2.5 V) (Figure 3d). Clearly, the presence of Pt remarkably enhances the catalytic effect of the electrode and the cycling performance of the battery, although the mass ratio of Pt to Co_3O_4 is only 1/39.

To understand the better catalytic activity of Pt/Co_3O_4 than bare Co_3O_4, the electrodes after discharge were observed by SEM and TEM, as shown in Figure 4. After discharge to 500 mAh g^{-1}, the Pt/Co_3O_4 electrode can maintain its pristine nanowires structure with bundled tips while the thickness of the nanowires is obviously increased (Figure 4a). The magnified view in Figure 4b indicates that the surface of the nanowires is coated with a thin layer of fluffy substance. The formation of the fluffy substance becomes more obvious on the tips of the nanowires because there several nanowires are bundled together (Figure 4b). The side view of the electrode (Figure S2) demonstrates that the discharge product deposits only on the periphery of Pt/Co_3O_4 nanowires without forming large deposits in between or on the top the nanowires. TEM image (Figure 4c) clearly reveals that the periphery of the Pt/Co_3O_4 nanowires is uniformly coated with a layer of fluffy substance. It seems that the fluffy substance is stacked from small and thin sheets. Selected area electron diffraction (SAED) confirms that the deposited surface layer is Li_2O_2 (Figure 4d).

As seen in Figure S3a, a thin layer composed of nanoparticles grows at the early discharge stage (200 mAh g^{-1}). As the discharge proceeds, the surface layer becomes thicker and looser with a fluffy morphology formed (Figure S3b). This may explain the two-step decomposition mechanism of Li_2O_2 mentioned above. As seen in Figure 4d, the polycrystalline feature of Pt/Co_3O_4 is preserved after discharge, which is further verified by HRTEM (Figure S3c). Li_2O_2 grows into dendritic form when the Pt/Co_3O_4 electrode is discharged to 1400 mAh g^{-1} (Figure S4). Note that no large Li_2O_2 deposits form even at this deep discharge state. After the fifth discharge, the original morphology of the Pt/Co_3O_4 electrode is well kept (Figure S5), indicating that the electrode can sustain repeated Li_2O_2 deposition/decomposition. Long-term cycling, however, leads to the deposition of large particles (2−20 μm) and the destruction of the Pt/Co_3O_4 electrode (Figure S6), which can explain the gradual degradation of battery performance after 50 cycles and the eventual failure of the battery after 56 cycles. The specific surface area decreases from 330 m^2g^{-1} in the pristine electrode to 128 m^2g^{-1} in the cycled electrode due to the destruction of the electrode. For bare Co_3O_4, the discharged electrode exhibits a rather different morphology. Large-sized flower-like particles (marked by A) and plate aggregates on nanowires (marked by B) can be clearly seen (Figure 4e). The enlarged view in domain C indicates that besides fluffy Li_2O_2, round Li_2O_2 plates also form on the nanowires (Figure 4f).

From the above results, we can see that Pt plays a critical role in changing the crystallization habit of Li_2O_2 although its content is rather low. For Pt/Co_3O_4, Pt can act as the nucleation sites for Li_2O_2 growth at the beginning of the discharge due to its superior oxygen absorption and ORR catalytic activities. Once the Li_2O_2 nanoparticles have formed, they can act as the nucleation centers for the continuous Li_2O_2 growth catalyzed by both Co_3O_4 and Pt. The homogeneous dispersion of Pt in Co_3O_4 nanowires ensures uniform growth of Li_2O_2 onto the periphery of Pt/Co_3O_4 nanowires. Due to the shielding effect of the deposited Li_2O_2, the catalytic effect of Pt may become weakened but it may be still active if the Li_2O_2 layer is not thick enough. This may direct the growth of Li_2O_2 into loosely stacked fluffy form. The thin, fluffy Li_2O_2 and its good contact with Pt/Co_3O_4 make it possible to decompose at low potentials, reducing high-potential related side reactions. Without the inducing effect of Pt, Li_2O_2 will grow into a large size and onto a random place on the electrode. The decomposition of Li_2O_2 upon recharge will become kinetically sluggish due to large size of Li_2O_2 and its poor contact with the catalyst, leading to high charge overpotentials and the accompanied side reactions. It becomes mechanically more stable for Pt/Co_3O_4 to support Li_2O_2 when the tips are bundled together. As a result, Pt/Co_3O_4 catalyzed Li−O_2 battery exhibits better electrochemical performance than the Co_3O_4 catalyzed one.

In summary, we fabricated an efficient binder/carbon-free catalytic cathode for Li−O_2 battery by growing tips-bundled Pt/Co_3O_4 nanowires directly on the 3D scaffold of Ni foam. Pt promotes the growth of Co_3O_4 nanowires in an orderly and tips-bundled fashion. The uniformly dispersed Pt nanocrystals direct the uniform growth of Li_2O_2 into thin, fluffy form, and only onto the periphery of the Pt/Co_3O_4 nanowires. This crystallization behavior of Li_2O_2 alleviates the passivation of the electrode and reduces the side reactions by decreasing the charge overpotentials. In contrast, in the Co_3O_4 cathode, Li_2O_2 grows into large particles with sluggish decomposition kinetics. As a result, Li−O_2 battery with Pt/Co_3O_4 cathode shows remarkably improved electrochemical performance compared with that with Co_3O_4 cathode. The Pt/Co_3O_4 catalyzed Li−O_2 battery can sustain a cycling over 50 times at a capacity of 500 mAh g^{-1}. The results also suggest that both the material and structure of the catalytic cathode should be optimized in order to achieve good electrochemical performance of Li−O_2 batteries

■ ASSOCIATED CONTENT

Ⓢ Supporting Information

The following file is available free of charge on the ACS Publications website at DOI: 10.1021/cs501392p.

Experimental section, and SEM/TEM images of the discharged electrodes (PDF)

■ AUTHOR INFORMATION

Corresponding Authors

*E-mail: (J.X.) xiejian1977@zju.edu.cn. Tel/Fax: +86-571-87951451.

*E-mail: (X.Z.) zhaoxb@zju.edu.cn.

Notes

The authors declare no competing financial interest.

■ ACKNOWLEDGMENTS

This work was supported by the National Basic Research Program of China (2013CB934001), the National Natural Science Foundation of China (No. 51101139), Key Science and Technology Innovation Team of Zhejiang Province under Grant Number 2010R50013, and Program for Innovative Research Team in University of Ministry of Education of China (IRT13037).

■ REFERENCES

(1) Abraham, K. M.; Jiang, Z. *J. Electrochem. Soc.* **1996**, *143*, 1−5.

(2) Ogasawara, T.; Débart, A.; Holzapfel, M.; Novák, P.; Bruce, P. G. *J. Am. Chem. Soc.* **2006**, *128*, 1390−1393.
(3) Bruce, P. G.; Freunberger, S. A.; Hardwick, L. J.; Tarascon, J. M. *Nat. Mater.* **2012**, *11*, 19−29.
(4) Lu, Y. C.; Gallant, B. M.; Kwabi, D. G.; Harding, J. R.; Mitchell, R. R.; Whittinghamd, M. S.; Shao Horn, Y. *Energy Environ. Sci.* **2013**, *6*, 750−768.
(5) Shao, Y. Y.; Park, S.; Xiao, J.; Zhang, J. G.; Wang, Y.; Liu, J. *ACS Catal.* **2012**, *2*, 844−857.
(6) Peng, Z. Q.; Freunberger, S. A.; Chen, Y. H.; Bruce, P. G. *Science* **2012**, *337*, 563−566.
(7) Shui, J. L.; Du, F.; Xue, C. M.; Li, Q.; Dai, L. M. *ACS Nano* **2014**, *8*, 3015−3022.
(8) Lim, H. D.; Song, H.; Kim, J.; Gwon, H.; Bae, Y.; Park, K. Y.; Hong, J.; Kim, H.; Kim, T.; Kim, Y. H.; Lepró, X.; Ovalle Robles, R.; Baughman, R. H.; Kang, K. *Angew. Chem., Int. Ed.* **2014**, *53*, 3926−3931.
(9) Viswanathan, V.; Thygesen, K. S.; Hummelshøj, J. S.; Nørskov, J. K.; Girishkumar, G.; McCloskey, B. D.; Luntz, A. C. *J. Chem. Phys.* **2011**, *135*, 214704.
(10) Xu, J. J.; Wang, Z. L.; Xu, D.; Zhang, L. L.; Zhang, X. B. *Nat. Commun.* **2013**, *4*, 2438.
(11) Lim, H. D.; Song, H.; Gwon, H.; Park, K. Y.; Kim, J.; Bae, Y.; Kim, H.; Jung, S. K.; Kim, T.; Kim, Y. H.; Lepró, X.; Ovalle Robles, R.; Baughman, R. H.; Kang, K. *Energy Environ. Sci.* **2013**, *6*, 3570−3575.
(12) Yilmaz, E.; Yogi, C.; Yamanaka, K.; Ohta, T.; Byon, H. R. *Nano Lett.* **2013**, *13*, 4679−4684.
(13) Black, R.; Oh, S. H.; Lee, J. H.; Yim, T.; Adams, B.; Nazar, L. F. *J. Am. Chem. Soc.* **2012**, *134*, 2902−2905.
(14) McCloskey, B. D.; Speidel, A.; Scheffler, R.; Miller, D. C.; Viswanathan, V.; Hummelshøj, J. S.; Nørskov, J. K.; Luntz, A. C. *J. Phys. Chem. Lett.* **2012**, *3*, 997−1001.
(15) Ottakam Thotiyl, M. M.; Freunberger, S. A.; Peng, Z. Q.; Bruce, P. G. *J. Am. Chem. Soc.* **2013**, *135*, 494−500.
(16) Gallant, B. M.; Mitchell, R. R.; Kwabi, D. G.; Zhou, J. G.; Zuin, L.; Thompson, C. V.; Shao Horn, Y. *J. Phys. Chem. C* **2012**, *116*, 20800−20805.
(17) Li, F. J.; Tang, D. M.; Chen, Y.; Golberg, D.; Kitaura, H.; Zhang, T.; Yamada, A.; Zhou, H. S. *Nano Lett.* **2013**, *13*, 4702−4707.
(18) Li, F. J.; Tang, D. M.; Jian, Z. L.; Liu, D. Q.; Golberg, D.; Yamada, A.; Zhou, H. S. *Adv. Mater.* **2014**, *26*, 4659−4664.
(19) Cui, Y. M.; Wen, Z. Y.; Liu, Y. *Energy Environ. Sci.* **2011**, *4*, 4727−4734.
(20) Ryu, W. H.; Yoon, T. H.; Song, S. H.; Jeon, S.; Park, Y. J.; Kim, I. D. *Nano Lett.* **2013**, *13*, 4190−4197.
(21) Black, R.; Lee, J. H.; Adams, B.; Mims, C. A.; Nazar, L. F. *Angew. Chem., Int. Ed.* **2013**, *52*, 392−396.
(22) Sun, B.; Zhang, J. Q.; Munroe, P.; Ahn, H. J.; Wang, G. X. *Electrochem. Commun.* **2013**, *31*, 88−91.
(23) Zhang, L. X.; Zhang, S. L.; Zhang, K. J.; Xu, G. J.; He, X.; Dong, S. M.; Liu, Z. H.; Huang, C. H.; Gu, L.; Cui, G. L. *Chem. Commun.* **2013**, *49*, 3540−3542.
(24) Débart, A.; Paterson, A. J.; Bao, J. L.; Bruce, P. G. *Angew. Chem., Int. Ed.* **2008**, *47*, 4521−4524.
(25) Truong, T. T.; Liu, Y. Z.; Ren, Y.; Trahey, L.; Sun, Y. G. *ACS Nano* **2012**, *6*, 8067−8077.
(26) Oh, D.; Qi, J. F.; Lu, Y. C.; Zhang, Y.; Shao Horn, Y.; Belcher, A. M. *Nat. Commun.* **2013**, *4*, 2756.
(27) Liu, S. Y.; Zhu, Y. G.; Xie, J.; Huo, Y.; Yang, H. Y.; Zhu, T. J.; Cao, G. S.; Zhao, X. B.; Zhang, S. C. *Adv. Energy Mater.* **2014**, *4*, 1301960.
(28) Zhang, W. Y.; Zeng, Y.; Xu, C.; Tan, H. T.; Liu, W. L.; Zhu, J. X.; Xiao, N.; Hng, H. H.; Ma, J.; Hoster, H. E.; Yazami, R.; Yan, Q. Y. *RSC Adv.* **2012**, *2*, 8508−8514.
(29) Radina, M. D.; Siegel, D. J. *Energy Environ. Sci.* **2013**, *6*, 2370−2379.
(30) McCloskey, B. D.; Bethune, D. S.; Shelby, R. M.; Mori, T.; Scheffler, R.; Speidel, A.; Sherwood, M.; Luntz, A. C. *J. Phys. Chem. Lett.* **2012**, *3*, 3043−3047.